SLAC-PUB-2024
October 1977
(T/E)

# RECENT RESULTS FROM SPEAR*

A.M. Litke

Department of Physics and Stanford Linear Accelerator Center
Stanford University, Stanford, California 94305

## I. Introduction

In this talk we will present recent experimental results from SPEAR on electron-positron annihilation reactions. The first result we will discuss (in Section II) is the observation of a new resonance in $e^+e^- \to$ hadrons.[1] This new state occurs at a center of mass energy of 3772 MeV and is thus just above the threshold for the production of charmed particles. We shall refer to this state as the $\psi(3772)$.

One of the special things about the $\psi(3772)$ is that it is a copious and clean source of D charmed mesons; the reaction $e^+e^- \to \psi(3772) \to D\bar{D}$ produces D's which have well-defined kinematics and little background. In Section III we give results, based on this reaction, on measurements of the $D^0$ and $D^+$ masses accurate to better than 1 MeV, on the observation of a new decay mode $D^- \to K_s^0\pi^-$, and on the D production angular distribution.[2]

The last topic we shall discuss (in Section IV) is the production of anomalous electrons. We will consider two-prong events of the type $e^+e^- \to e^\pm\mu^\mp$ or $e^\pm(\text{hadron})^\mp$, with or without additional photons, and also multi-prong events of the form $e^+e^- \to e^\pm$ + two or more charged particles, with or without additional neutrals. The two-prong data will be compared to the results expected from the production and decay of a pair of heavy leptons. Assuming these events come only from this source we calculate the branching ratios $B(\tau^- \to e^-\bar{\nu}_e\nu_\tau)$ and $B(\tau \to$ charged hadron + neutrals$)$.[3] The

---

*Work supported in part by the Department of Energy.
(Invited talk presented at the European Conference on Particle Physics, July 4-9, 1977, Budapest, Hungary.)

multiprong sample, particularly from the $\psi(3772)$, will be used to derive a value for the semi-leptonic branching ratio of the D meson.

The results presented here are due to the work of the Lead Glass Wall Collaboration.[4] The data were collected with the SLAC-LBL Mark I magnetic detector[5] to which had been added a lead glass detector[3] which covers a part of the solid angle (see Figure 1 for a view of the apparatus along the beam line). The lead glass system is used for the detection of electrons, photons and neutral pions and will be discussed in Section IV.

The data sample has been divided into four center of mass energy ranges: 3.76-3.79, 4.15, 4.4-5.7, and 6.4-7.4 GeV. Table I lists the average energy, the integrated luminosity, and the total number of detected hadron events for each energy region.

TABLE I

Average center of mass energy ($\bar{E}_{c.m.}$), integrated luminosity ($\int Ldt$), and the number of detected hadron events ($N_{had}$) for each of four center of mass energy ranges.

| Center of Mass Energy Range (GeV) | $\bar{E}_{c.m.}$ (GeV) | $\int Ldt$ ($pb^{-1}$) | $N_{had}$ |
|---|---|---|---|
| 3.76 - 3.79 | 3.77 | 1.2 | 25,000 |
| 4.15 | 4.15 | 1.0 | 16,000 |
| 4.4 - 5.7 | 4.9 | 2.5 | 32,000 |
| 6.4 - 7.4 | 6.9 | 5.1 | 44,000 |

We mention two reports in these proceedings with experimental results closely related to those presented here: Goldhaber summarizes the experi-

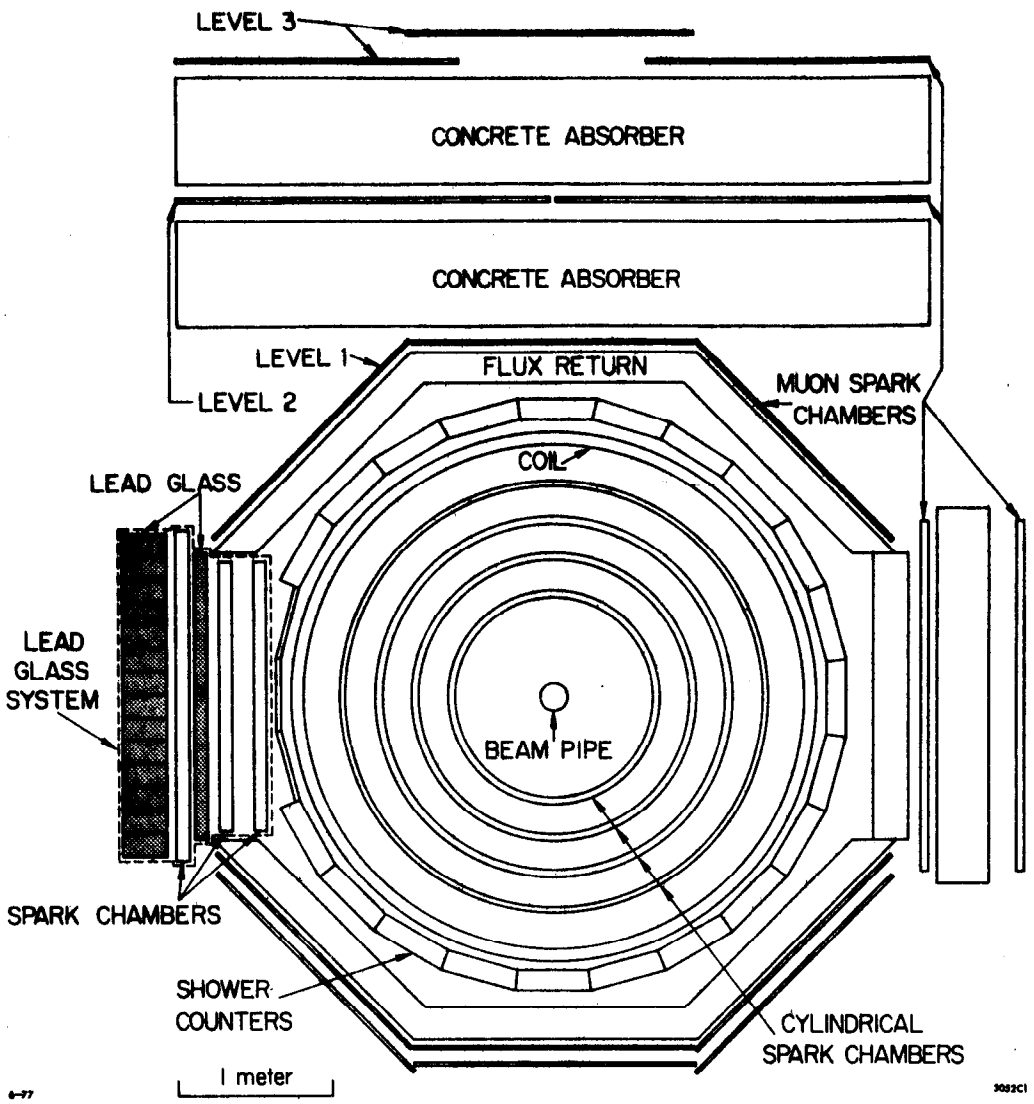


Fig. 1. The Mark I magnetic detector with the lead glass wall add-on in a view along the beam line. The two proportional chambers around the beam pipe and the trigger counters are not shown.

mental data on the D and $D^*$, and Timm reviews the recent experimental results from DORIS.

## II. Observation of a New Resonance in $e^+e^- \to$ hadrons: the $\psi(3772)$

Until quite recently there has been a sparsity of data on the total cross section for $e^+e^-$ annihilation into hadrons ($\sigma_{had}$) in the center of mass energy region between the $\psi(3684)(\equiv\psi')$ and 3.9 GeV.[6] In the past month at SPEAR we have been running in this energy region in order to obtain measurements of $\sigma_{had}$ with high statistics. The results are shown in Figure 2 where we have plotted the ratio R of $\sigma_{had}$ to the theoretical cross section ($\sigma_{\mu\mu}$) for $e^+e^- \to \mu^+\mu^-$. Figure 2a shows R <u>before</u> the application of radiative corrections.[7] We observe a resonant structure at about 3.77 GeV with a shape distorted somewhat by the radiative tail of the $\psi'$.

This data must be corrected for radiative effects in the initial state. These corrections take account of the $\psi'$, the $\psi(3095)$, the resonant structure at 3.77 GeV, and the continuum.[1] The corrected values of R are plotted in Figure 2b. To show how the resonance at 3.77 GeV fits into the R landscape we plot in Figure 3 the data of Figure 2b along with a point at 3.6 GeV and previous measurements[8,9] of R from the SLAC-LBL Collaboration (taken also in the Mark I detector).

In order to evaluate quantitatively the parameters of the resonant peak around 3.77 GeV, we have fit the radiatively corrected data to a Breit-Wigner expression plus a background term. One acceptable fit ($\chi^2 = 16.9$ for 15 degrees of freedom) is shown in Figure 2b. The curve is given by:

$$R = \frac{\sigma_{had}}{\sigma_{\mu\mu}} = R_{BW} + R_{BG} \qquad \text{(II.1)}$$

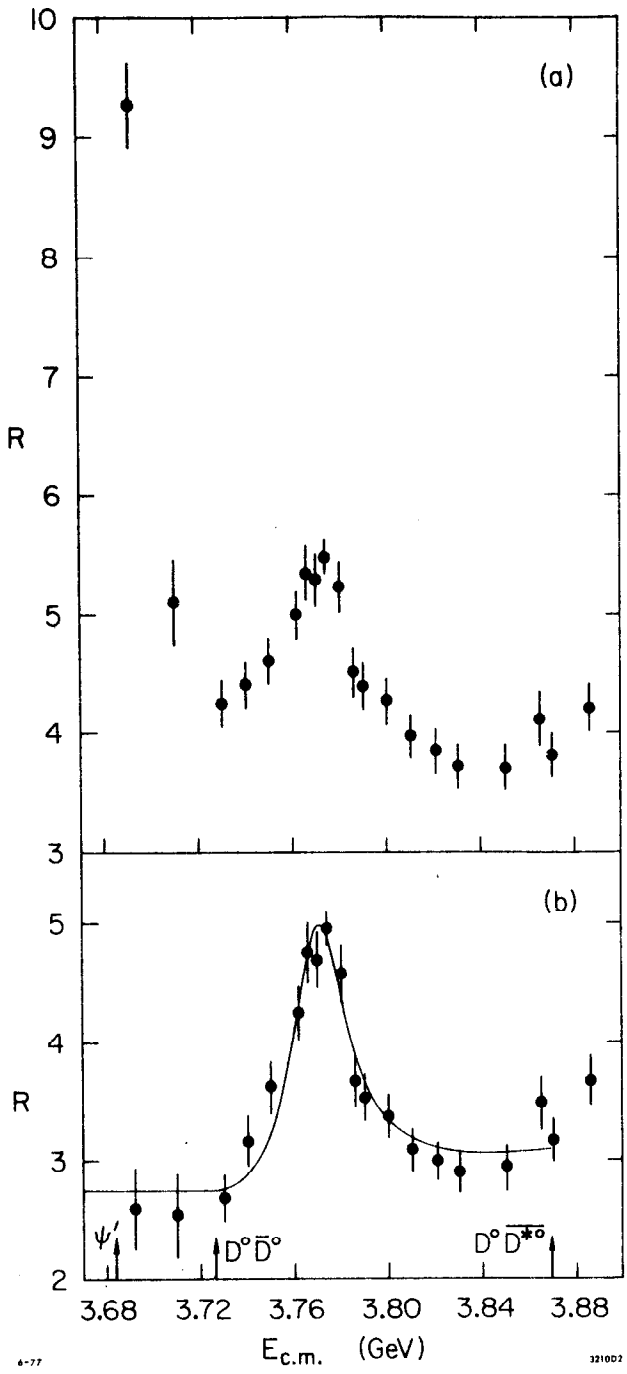


Fig. 2. R vs. $E_{c.m.}$ (a) before and (b) after radiative corrections. The curve is described in the text.

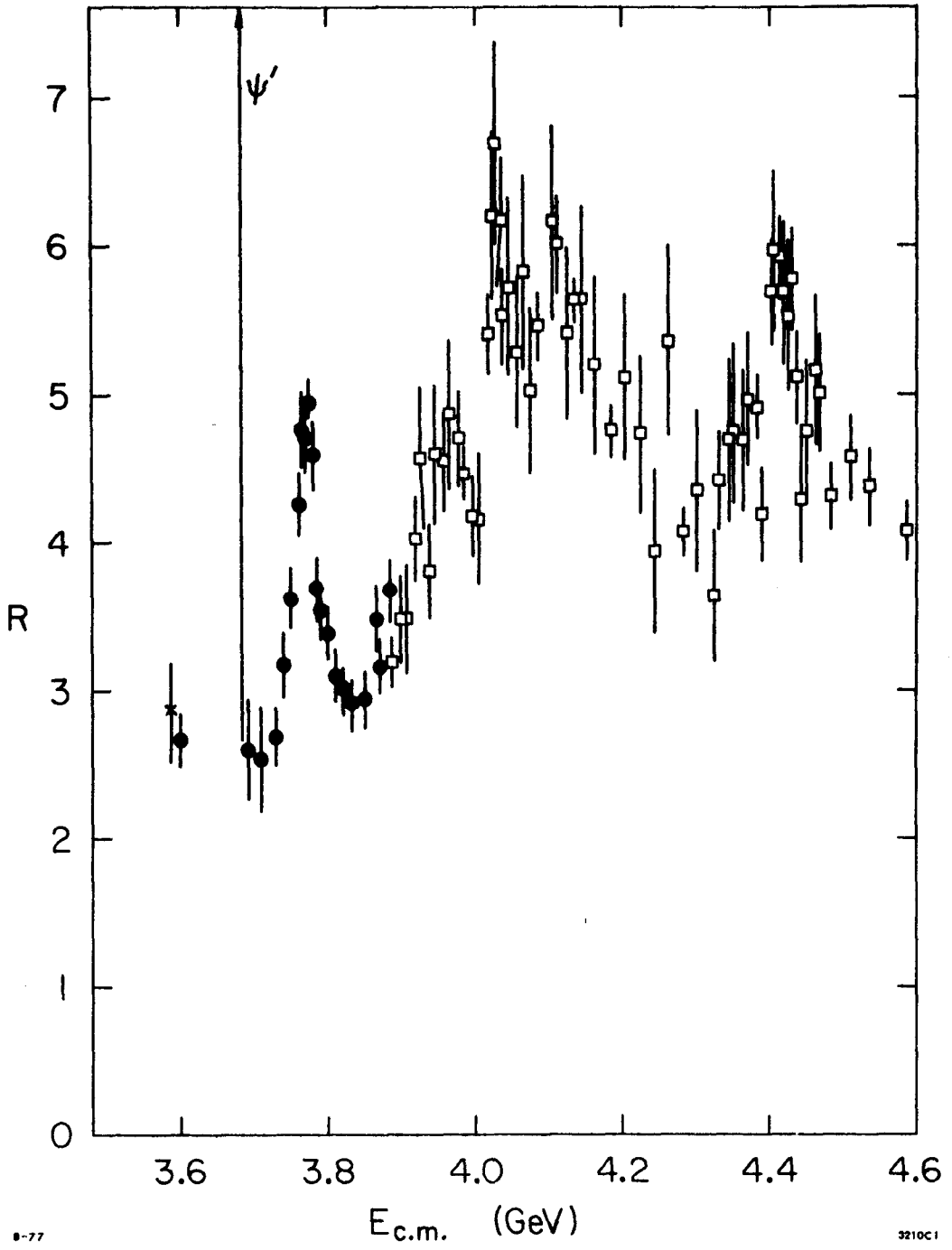


Fig. 3. Radiatively corrected values of R vs. $E_{c.m.}$. The closed circles are from Ref. 1, the open squares are from Ref. 8, and the crossed point is from Ref. 9.

with

$$R_{BW} = \frac{3\pi}{\sigma_{\mu\mu} M^2} \frac{\Gamma_{ee}\Gamma(E_{c.m.})}{(E_{c.m.} - M)^2 + \Gamma^2(E_{c.m.})/4} \qquad \text{(II.2)}$$

where M is the mass of the resonance, $\Gamma_{ee}$ is the partial width to $e^+e^-$, and $\Gamma(E_{c.m.})$ is the total width which is a function of the center of mass energy $E_{c.m.}$ As we shall see in Section III, the resonance decays copiously into $D\bar{D}$ so it is appropriate to take an energy dependence for $\Gamma$ which includes a p wave barrier factor:[10]

$$\Gamma(E) \propto \frac{p_o^3}{1 + (rp_o)^2} + \frac{p_+^3}{1 + (rp_+)^2} \qquad \text{(II.3)}$$

with $p_o$ and $p_+$ the momenta, respectively, of the $D^o$ and $D^+$ coming from D pair production and r an interaction radius (for the fit shown, r = 3 fm. but acceptable fits are obtained for any value of $r > 1$ fm.). The background term $R_{BG}$ is not critical and was taken for this fit to be a constant plus a constant times $(p_o^3 + p_+^3)$.

The parameters for the $\psi(3772)$ based on this fit, with errors which take into account the uncertainty in the form of the fitting function, are given in Table II. Also given are the previously measured parameters of the other isolated $\psi$ resonances.[8,11,12]

TABLE II

Resonance parameters for the isolated $\psi$ resonances. $\Gamma$ is the full width, $\Gamma_{ee}$ is the partial width to electron pairs, and $B_{ee}$ is the branching fraction to electron pairs. Errors on the mass include a 0.13% uncertainty in the absolute energy calibration of SPEAR. The mass difference between the $\psi(3684)$ and $\psi(3772)$ is $88 \pm 3$ MeV/$c^2$.

| State | Mass (MeV/$c^2$) | $\Gamma$ (MeV/$c^2$) | $\Gamma_{ee}$ (keV/$c^2$) | $B_{ee}$ |
|---|---|---|---|---|
| $\psi(3095)$ | $3095 \pm 4$ | $0.069 \pm 0.015$ | $4.8 \pm 0.6$ | $0.069 \pm 0.009$ |
| $\psi(3684)$ | $3684 \pm 5$ | $0.228 \pm 0.056$ | $2.1 \pm 0.3$ | $(9.3 \pm 1.6) \times 10^{-3}$ |
| $\psi(3772)$ | $3772 \pm 6$ | $28 \pm 5$ | $0.37 \pm 0.09$ | $(1.3 \pm 0.2) \times 10^{-5}$ |
| $\psi(4414)$ | $4414 \pm 7$ | $33 \pm 10$ | $0.44 \pm 0.14$ | $(1.3 \pm 0.3) \times 10^{-5}$ |

One possible interpretation of the $\psi(3772)$ is that it is the $^3D_1$ state of charmonium. Indeed, Lane and Eichten,[13] updating the calculations of Eichten et al.[14] to take account of the measured $D^o$ mass, predicted over one year ago the existence of a $^3D_1$ charmonium state with a mass of 3.77 GeV, a total width equal to that of the $\psi(3772)$, and a value for $\Gamma_{ee}$ about a factor of two lower than the measured value for $\psi(3772)$. If the $\psi(3772)$ is a state of charmonium then it should decay, with normal hadronic width, into the Zweig-allowed channel $D\bar{D}$. In the next section we shall demonstrate the existence of this decay mode.

For a detailed summary of the charmonium model the reader should consult the report of Jackson in these proceedings.

## III. Study of D Mesons from $\psi(3772) \to D\bar{D}$

### A. D Production; $D^{\pm} \to K_s \pi^{\pm}$

The $\psi(3772)$ lies below the threshold for $D\bar{D}^*$ (3869 MeV) or $D\bar{D}\pi$ (3861 MeV) production. Thus in the region of this resonance D's can only be produced in the pair production reaction $e^+e^- \to D\bar{D}$. Each D meson must have an energy equal to the beam energy $E_B = E_{c.m.}/2$ and the D mass m can be evaluated from the total momentum p of its decay products according to the equation:

$$m = \sqrt{E_B^2 - p^2} \quad . \qquad \text{(III.1)}$$

This kinematic constraint is useful for reducing the background relative to the D signal and for improving the mass resolution.

In Figure 4 we plot the mass value given by equation III.1 for particle combinations in multihadronic events corresponding to five decay modes of the D. For these plots the center of mass energy is restricted to the range 3.76 to 3.79 GeV. Time of flight is used to identify $K^{\pm}$ and $\pi^{\pm}$.[15] Neutral kaons are identified by measurement of the $\pi^+\pi^-$ invariant mass and by consistency of the dipion momentum at the decay vertex with the kaon line of flight.[16] A particle combination, with a particle type assigned to each track, is plotted only if the total energy of the particles is within 50 MeV of the beam energy.

There is a clear D signal in each of the five modes, demonstrating the existence of the $\psi(3772) \to D\bar{D}$ decay mode. We observe the decay $D^{\pm} \to K_s \pi^{\pm}$, reported here for the first time. With efficiencies taken into account we find $B(D^+ \to \bar{K}^0\pi^+)/B(D^+ \to K^-\pi^+\pi^+) = 0.39 \pm 0.15$.

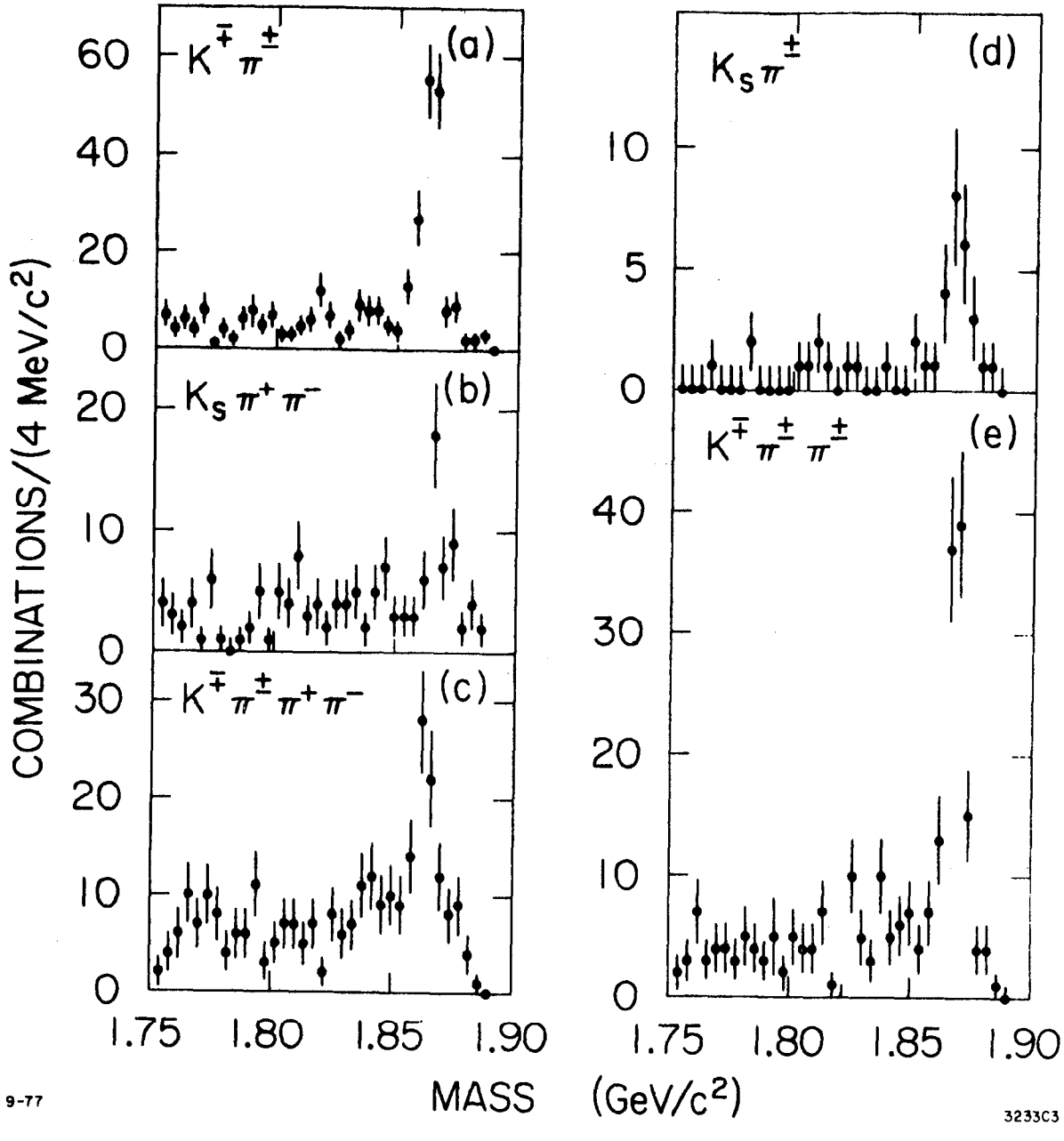


Fig. 4. Mass spectra at the $\psi(3772)$ for five D decay modes.

B. $D^o$ and $D^+$ Masses

The calculation of the D mass with equation III.1 implicitly constrains the total energy of the decay products of the D to equal the beam energy. As the spread in the beam energy[17] is much smaller than the spread in the measured total energy of the particles, this constraint improves the mass resolution by a factor of five to ten over a mass calculation based on the measured energy. In addition, the small value of p (about 300 MeV/c) implies that the error in the mass due to the error in p will be small. Overall, we expect an rms mass resolution of about 3 MeV/$c^2$ which is consistent with the data shown in Figure 4.

In Figure 5 we plot the $D^o$ and $D^+$ mass spectra, combining all observed decay modes, in 2 MeV/$c^2$ bins. Mass values for the $D^o$ and $D^+$ may be obtained by fitting this data. We find:

$$M_{D^o} = 1863.3 \pm 0.9 \text{ MeV}/c^2$$

and

$$M_{D^+} = 1868.3 \pm 0.9 \text{ MeV}/c^2 \quad .$$

The quoted errors include statistical (0.3 to 0.4 MeV/$c^2$) and systematic (0.8 MeV/$c^2$) contributions with the major systematic uncertainties coming from the absolute momentum calibration (0.5 MeV/$c^2$) and from the long term monitoring of $E_B$ (0.5 MeV/$c^2$). These errors do not include a 0.13% uncertainty in the absolute energy calibration of SPEAR. The D mass values are thus relative to the mass of the $\psi$ with the $\psi$ mass taken to be 3095 MeV/$c^2$.

The $D^+$-$D^o$ mass difference is determined more accurately than the individual masses due to the cancellation of several systematic errors. We find:

$$M_{D^+} - M_{D^o} = 5.0 \pm 0.8 \text{ MeV}/c^2 \quad .$$

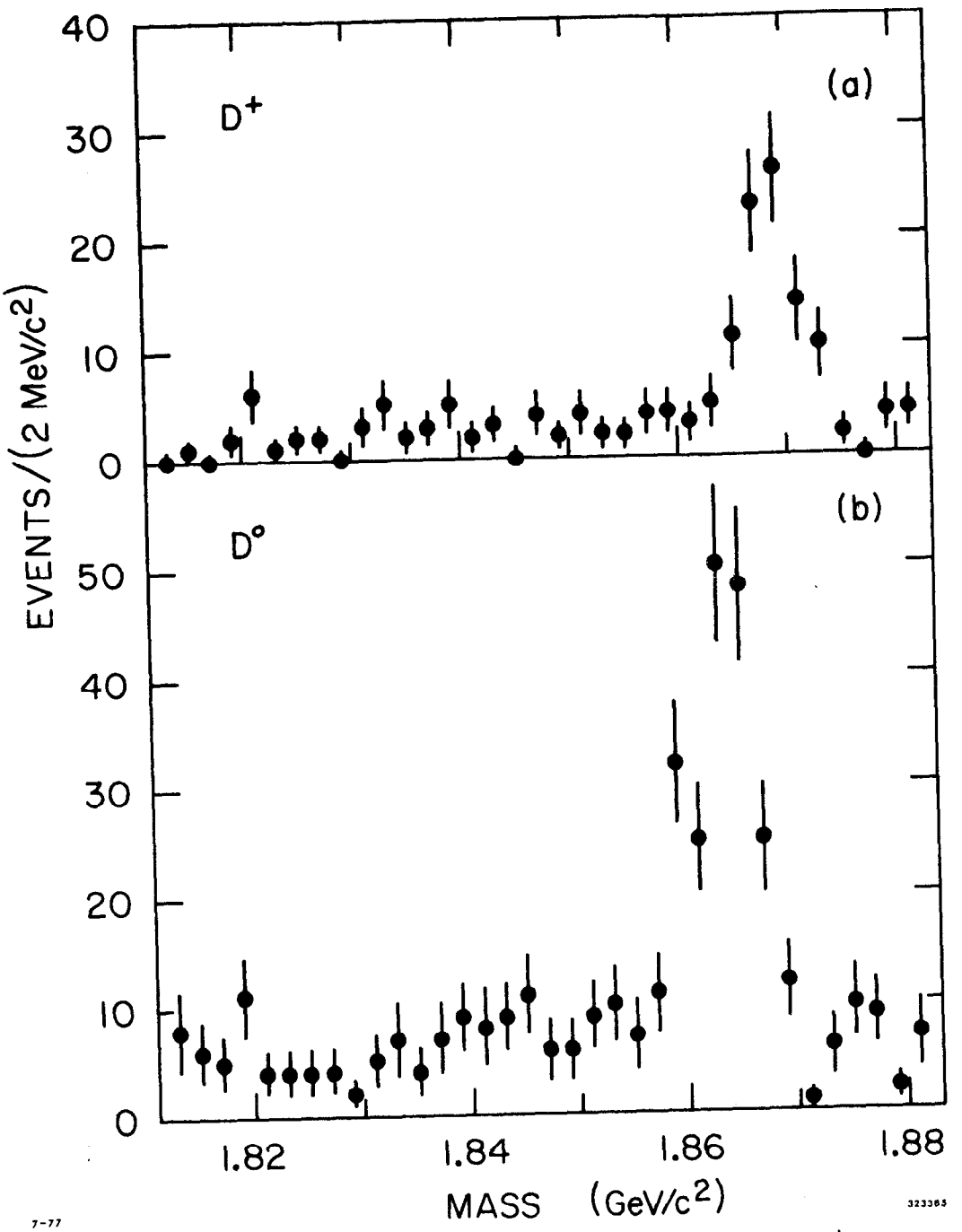


Fig. 5. Mass spectra at the $\psi(3772)$ for $D^{\pm}$ into $K_S\pi^{\pm}$ and $K^{\mp}\pi^{\pm}\pi^{\pm}$ and for $D^0(\overline{D^0})$ into $K^{\mp}\pi^{\pm}$, $K_S\pi^+\pi^-$, and $K^{\mp}\pi^{\pm}\pi^+\pi^-$.

For a discussion of the $D^*$ masses and $D^* \to D\pi$ Q values see the report of Goldhaber in these proceedings.

C. D Angular Distributions

The electromagnetic coupling (at lowest order) requires that at high center of mass energies the $e^+e^-$ system has J = 1 and $J_z = \pm 1$ where the z axis is taken to lie along the beam direction. Thus if the D mesons are spinless the angular distribution for the D's produced in the reaction $e^+e^- \to D\bar{D}$ must behave like $\left|Y_1^{\pm 1}(\theta,\phi)\right|^2 \propto \sin^2\theta$. In Figure 6 we show the production angular distributions for $D^o \to K^-\pi^+$ and $D^+ \to K^-\pi^+\pi^+$. They are seen to be consistent with the hypothesis of zero spin for the D mesons.[18]

IV. Anomalous Electron Production

A. Sources of Anomalous Electrons

To set the stage for this section, we remind the reader of the following two possible sources of anomalous electron production in electron-positron reactions:

(1) Heavy Lepton ($\tau$) Production and Decay

For example:

$$e^+e^- \to \tau^+\tau^- \qquad \tau^- \to e^-\bar{\nu}_e\nu_\tau \quad . \qquad \text{(IV.1)}$$

Evidence for the $\tau$ was first uncovered in the $e\mu$ events of Perl.[19,20] These early results have been confirmed and extended[21] at both SPEAR[22-25,3] and DORIS.[26-28] The decay modes and branching ratios predicted for a lepton with mass $M(\tau) = 1.9\ \text{GeV}/c^2$, $M(\nu_\tau) = 0$, and V-A weak interaction coupling[29] are shown in Table III.[30] About 85% of $\tau$ decays are expected to yield only a single charged particle. Thus about 85% of the events of type IV.1 will produce only two charged prongs in the final state.

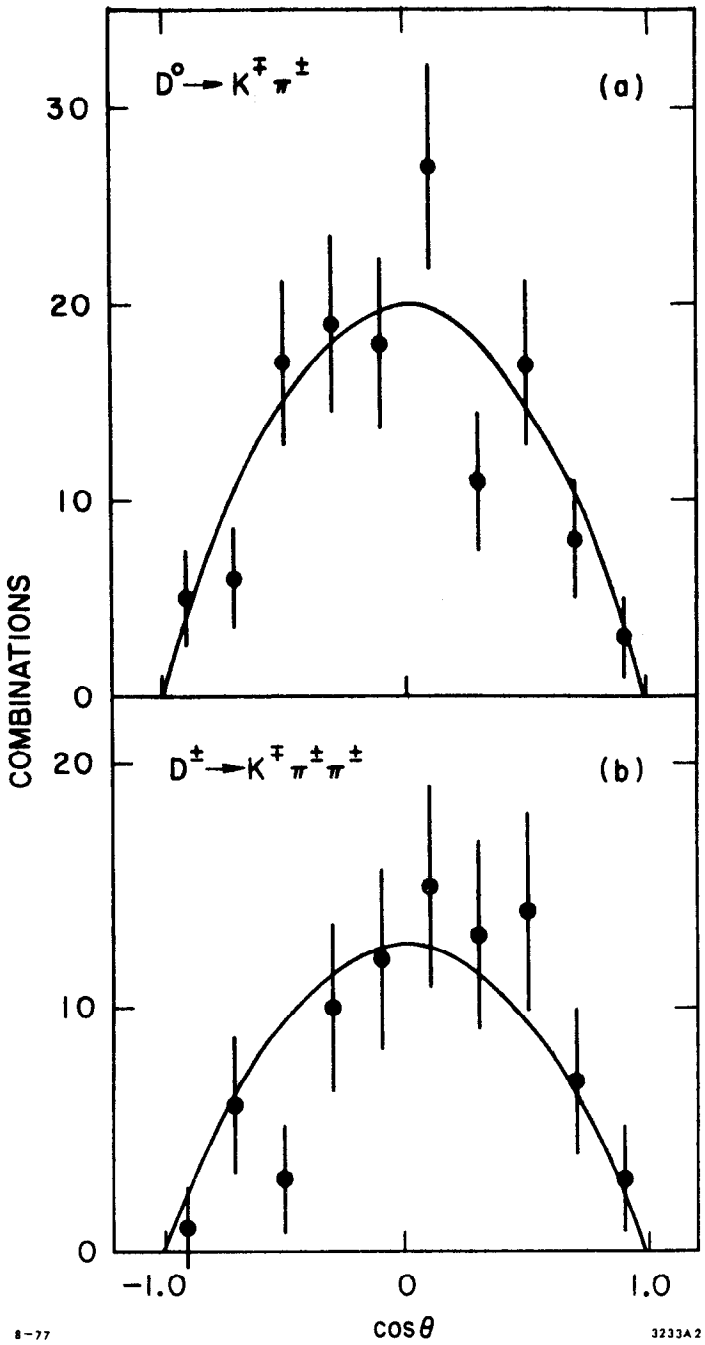


Fig. 6. Production angular distribution for a) $D^0(\bar{D}^0) \to K^\mp\pi^\pm$ and b) $D^\pm \to K^\mp\pi^\pm\pi^\pm$. $\theta$ is the angle between the $e^+$ beam direction and the D momentum. The curves represent the expected $\sin^2\theta$ distribution for spinless D mesons.

TABLE III

Predicted branching ratios for a $\tau^-$ charged lepton with a mass 1.9 GeV/$c^2$, an associated neutrino mass of 0.0, and V-A weak interaction coupling.[30]

| decay mode | branching ratio | number of charged particles in final state |
|---|---|---|
| $\nu_\tau e^- \bar{\nu}_e$ | .20 | 1 |
| $\nu_\tau \mu^- \bar{\nu}_\mu$ | .20 | 1 |
| $\nu_\tau \pi^-$ | .11 | 1 |
| $\nu_\tau K^-$ | .01 | 1 |
| $\nu_\tau \rho^-$ | .22 | 1 |
| $\nu_\tau K^{*-}$ | .01 | 1 |
| $\nu_\tau A_1^-$ | .07 | 1, 3 |
| $\nu_\tau$(hadron continuum)$^-$ | .18 | 1, 3, 5 |

(2) Charmed Particle Production and Decay

For example:

$$e^+e^- \rightarrow D\bar{D} + \text{possibly other hadrons}$$
$$\hookrightarrow e^- \bar{\nu}_e \text{ (K or } K^*\text{)} \qquad \text{(IV.2)}$$

An anomalous electron signal[31] and an electron-$K_s$ correlation,[32] possibly arising from charm decay, have been seen at DORIS.[28] We expect that most of the time events of the type IV.2 will produce more than two charged prongs in the final state.

The two sources listed above will provide a framework for the interpretation of our experimental results. As indicated, heavy lepton production will yield mainly two-prong events, and anomalous electron events due to charm will produce mainly multiprong events. It is therefore convenient for us to analyze our data separately for the two-prong and multiprong categories. This is a first order attempt at separating the charm → e signal from the $\tau \rightarrow e$ signal.

B. The Identification of Electrons in the Lead Glass Wall

One of the major experimental problems in the measurement of the anomalous electron signal is the identification of electrons in a large background flux of hadrons. To perform this identification we have used a lead glass system which covers about 10% of the solid angle of the Mark I detector (see Figure 1). This lead glass detector consists of:

(1) a 2 × 26 array of lead glass active converters, $3X_o$ deep (dimensions $10 \times 11 \times 90$ cm$^3$),

(2) a 14 × 19 array of lead glass "back blocks", 10 $X_o$ deep (dimensions $15 \times 15 \times 32$ cm$^3$), and

(3) a set of three magnetostrictive spark chambers (for shower position information).

This lead glass wall subtends the polar angles $60^{o} < \theta < 120^{o}$ and azimuthal angles $-20^{o} < \phi < 20^{o}$.

The energy calibration of the lead glass system uses electrons of known energy from Bhabha scattering. The response of the lead glass wall to Bhabha electrons is shown in Figure 7. The energy resolution is given by $\sigma/E \simeq 9\%/\sqrt{E}$ (particle energy E in GeV). This resolution is degraded from $5\%/\sqrt{E}$ due to the presence of the 1 $X_o$ aluminum coil of the Mark I magnet which precedes the lead glass wall.

The identification of particles that enter the lead glass system is based on the energy deposited in the active converter counters ($E_{AC}$) and on the energy deposited in the back block counters ($E_{BB}$). The criteria for identifying a particle as an electron are:

(1) The total energy deposited in the lead glass system $E_{TOT} = E_{AC} + E_{BB}$ is approximately equal to the particle momentum p as measured in the Mark I detector,

(2) The amount of energy deposited in the active converters is substantially greater than the 80 MeV expected for a non-interacting particle, and

(3) A significant amount of energy is deposited in the back blocks. (This criterion is used only for the multiprong analysis.)

In our analysis at this time we restrict ourselves to particle momenta greater than 400 MeV/c to insure a clean separation between electrons and hadrons.

For both the two-prong and multiprong analyses, we show in Table IV the cuts used to identify an electron, the average electron identification efficiency ($\epsilon$), and the average probability that a hadron is identified as an electron ($P_{h \to e}$). The measurement of $\epsilon$ is based on a sample of electrons from the reactions $e^+e^- \to e^+e^-\gamma$ and $e^+e^-e^+e^-$. $P_{h \to e}$ has been measured

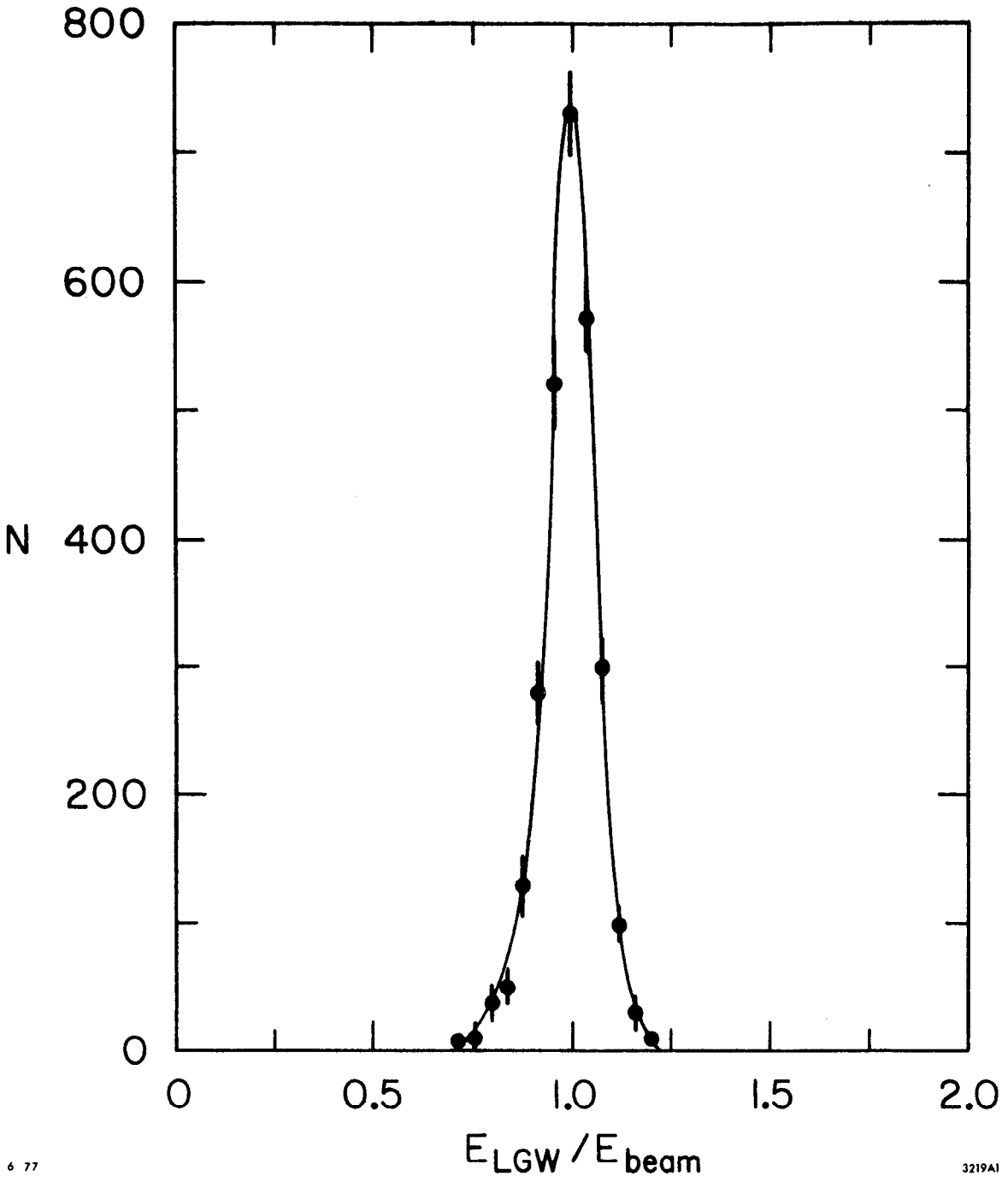


Fig. 7. Distribution of the total energy measured in the lead glass wall ($E_{LGW}$) divided by the beam energy for electrons from the reaction $e^+e^- \rightarrow e^+e^-$. The beam energy is 3.2 GeV. The energy resolution is $\sigma_{E_{LGW}}/E_{LGW} = 5.1\%$.

using multihadronic events from $\psi$ decay. (We assume there is no anomalous electron signal at the $\psi$.) The specific criteria for identifying an electron are more restrictive for the multiprong sample than for the two-prong sample since the hadronic background relative to the signal is much greater in the multiprong events.

TABLE IV

Lead glass wall electron identification criteria, average electron identification efficiency ($\epsilon$) and average probability that a hadron is identified as an electron ($P_{h \to e}$). $E_{AC}$ is the energy measured in the active converters, $E_{BB}$ is the energy measured in the back blocks, $E_{TOT} = E_{AC} + E_{BB}$, and p is the particle momentum (expressed in GeV).

| | Two Prong Analysis | Multiprong Analysis |
|---|---|---|
| $E_{TOT}/p$ cut | $0.65 < E_{TOT}/p < 1.5$ | $E_{TOT}/p > \text{Min}[0.8, 0.65 + 0.15(p-0.4)]$ and $E_{TOT}/p < 1.5$ |
| $E_{AC}$ cut | $E_{AC} > 0.15$ GeV | $E_{AC} > \text{Max}[0.15 \text{ GeV}, 0.25\ p]$ |
| $E_{BB}$ cut | --- | $E_{BB} > 0.1\ p$ |
| $\epsilon$ | 89% | 79% |
| $P_{h \to e}$ | 1.7% | 0.7% |

An important source of background for the anomalous electron signal is $\gamma$ conversion or Dalitz decay in which one member of the $e^+e^-$ pair has a low momentum and is therefore undetected. This background can be expressed as an increase in the values of $P_{h \to e}$ quoted in Table IV by about 0.3%. This number is determined by measuring $e^+e^-$ pairs with both particles detected, then extrapolating to the case of pairs with one low momentum e.

C. Two-Prong Events

We now consider the sample of events in which two charged particles of opposite electric charge are observed in the detector, and at least one of these particles is detected in the lead glass wall. (Only analysis of the energy regions 4.15, 4.4-5.7 and 6.4-7.4 GeV will be discussed here. Analysis of the $\psi(3772)$ data has not yet been completed.) We further select our events with the following criteria:

(1) The momentum of the particle in the lead glass wall must be greater than 400 MeV/c.

(2) The momentum of the other detected particle must be greater than 650 MeV/c.

(3) The two prongs must be acoplanar about the incident beams by at least $20^\circ$.

(4) The square of the missing mass recoiling against the two prongs must be greater than 0.8, 1.1, or 1.5 $GeV^2$ for the $E_{c.m.}$ range 4.15, 4.4-5.7, or 6.4-7.4 GeV, respectively.

Criteria (1) and (2) insure good particle indentification in the lead glass wall and in the Mark I detector. Criteria (3) and (4) reduce substantially

the background from the QED reactions

$$e^+e^- \to e^+e^-,\ e^+e^-\gamma \text{ and } e^+e^-e^+e^- \ .$$

Particle identification in the Mark I detector is based on pulse height in the lead-scintillator shower counters and on penetration through the 20 cm thick iron flux return of the magnet. The misidentification probabilities $P^D$ and identification efficiencies $\epsilon^D$ for the Mark I detector are measured with ee$\gamma$ events, $\mu\mu\gamma$ events, and hadronic events with 5 or more charged prongs. We find $P^D_{e \to h} = 9.5\%$, $P^D_{e \to \mu} = 1\%$, $P^D_{\mu \to h} = 3\%$, $P^D_{h \to \mu} = 18\%$, $\epsilon^D(e) = 89\%$, $\epsilon^D(h) = 58\%$, and $\epsilon^D(\mu) = 94\%$. These values are averages over the observed momentum spectrum; h represents a hadron.

The two-prong events which pass our cuts are shown in Table V. They are listed according to (1) the identity of the particle in the lead glass wall ("e" if it passes the electron cuts; "no e" otherwise), (2) the identity of the other prong, and (3) whether or not there are any neutrals detected in the event (the notation "$\gamma$" means that one or more neutrals are detected in the lead-scintillator shower counters or in the lead glass wall). The anomalous electron events of interest to us are in the categories e$\mu$, eh, e$\mu\gamma$ and eh$\gamma$. The expected background for these events due to misidentification of ee, (no e) h, ee$\gamma$, and (no e) h$\gamma$ events is shown in column 3. The last column lists the number of anomalous events after corrections for the background listed in column 3, the misidentifications among the anomalous events themselves, and the particle identification efficiencies.

TABLE V

Two-Prong Events

Combined data from $E_{c.m.}$ = 4.15, 4.4-5.7, and 6.4-7.4 GeV. See text for event selection criteria.

| Event Category (The first particle listed is identified in the lead glass wall) | Number of Observed Events | Expected Background from ee, ee$\gamma$, (no e)h, and (no e)h$\gamma$ Events | Corrected # of Events |
|---|---|---|---|
| e$\mu$ | 21 | 0.4 | 21.6 ± 6.4 |
| eh | 12 | 3.0 | 20.5 ± 9.6 |
| e$\mu\gamma$ | 8 | 1.4 | 3.7 ± 4.5 |
| eh$\gamma$ | 19 | 9.1 | 24.2 ± 12.9 |
| ee | 23 | | |
| (no e)h | 38 | | |
| ee$\gamma$ | 71 | | |
| (no e)h$\gamma$ | 122 | | |

There are 21 eμ events detected with a calculated background of only 0.4 events from conventional sources and 31 eh and ehγ events detected with a background of 12.1.[33] We attribute the events above background to a nonconventional process.

Next we interpret this anomalous electron signal in the two-prong events in the framework discussed in Section IV.A and hypothesize that these events arise from the production and decay of a heavy lepton. To be specific we take the properties of the heavy lepton to be:

$$M(\tau) = 1.9 \text{ GeV}/c^2$$

$$M(\nu_\tau) = 0 \qquad \text{IV.3}$$

V-A weak interaction coupling

These properties are consistent with previous measurements.[19-27] Below we check the consistency of the heavy lepton hypothesis with our data.

eμ Events

We assume the eμ events are produced by the process:

$$e^+e^- \to \tau^+\tau^- \quad \begin{cases} \to e^-\bar{\nu}_e\nu_\tau \\ \to \mu^+\nu_\mu\bar{\nu}_\tau \end{cases} \qquad \text{(IV.4)}$$

Then the observed cross section $\sigma(e\mu)$ is given by:

$$\sigma(e\mu) = 2\, A_{e\mu}\, \sigma(\tau^+\tau^-)\, B_e B_\mu \qquad \text{(IV.5)}$$

where $A_{e\mu}$ is the acceptance of the apparatus for the eμ events, $\sigma(\tau^+\tau^-)$ is the point-like cross section for $e^+e^- \to \tau^+\tau^-$, and $B_e(B_\mu)$ is the branching ratio for $\tau \to e\nu_e\nu_\tau(\mu\nu_\mu\nu_\tau)$. Given the properties for τ assumed in IV.3 we can calculate $A_{e\mu}$ and $\sigma(\tau^+\tau^-)$. Then assuming $B_e = B_\mu$ we calculate $B_e$ from our data. The results are given in Table VI for three

energy regions.

TABLE VI

Measured branching ratios $B_e$ for $\tau \to e\nu_e\nu_\tau$ and $B_h$ for $\tau \to$ single charged hadron + neutrals. The assumptions used in deriving these results are described in the text. Only statistical errors are shown.

| Center of Mass Energy Region (GeV) | $B_e$(%) | $B_h$(%) |
|---|---|---|
| 4.15 | 21.3 ± 8.5 | 37 ± 43 |
| 4.4 - 5.7 | 20.4 ± 5.4 | 50 ± 29 |
| 6.4 - 7.4 | 24.1 ± 4.6 | 45 ± 26 |

The agreement between the three values of $B_e$ shows that the energy dependence of $e\mu$ production is consistent with the heavy lepton hypothesis. Combining the data and including an estimated 20% systematic error we obtain $B_e = (22.4 \pm 5.5)\%$. This value is in agreement with previous measurements[19,25,26] and with the theoretical expectation of 20%.[34]

eh and ehγ Events

We assume these events are produced by the reaction:

$$e^+e^- \to \tau^+\tau^- \quad \begin{cases} \to e^-\bar{\nu}_e\nu_\tau \\ \to \bar{\nu}_\tau + \text{single charged hadron} + \text{possibly additional neutrals} \end{cases} \qquad \text{(IV.6)}$$

then:

$$\sigma(eh,\ eh\gamma) = 2\, A_{eh}\, \sigma(\tau^+\tau^-)\, B_e\, B_h \qquad \text{(IV.7)}$$

where $A_{eh}$ is the acceptance for eh and ehγ events and $B_h$ is the branching

ratio for $\tau \rightarrow$ single charged hadron + neutrals. We assume properties IV.3 for $\tau$. In addition, for the calculation of $A_{eh}$, we take as a model the decays $\tau \rightarrow \pi\nu_\tau$ and $\tau \rightarrow \rho\nu_\tau$. (We expect these decay modes to constitute 73% of the $\tau \rightarrow$ single charged hadron decays.) With the value of $B_e$ quoted above and with our measurements of $\sigma(eh, eh\gamma)$ we evaluate $B_h$ as shown in Table VI. We find $B_h = (45 \pm 19)\%$, in agreement with the theoretical expectation of 45%.[34]

Momentum and Coplanarity Distributions

Figure 8(a)-8(c) shows the corrected momentum distributions for (a) the hadrons, (b) the muons, and (c) the electrons in the $e\mu$, $eh$, and $eh\gamma$ events. The momentum distributions are given in terms of the variable r defined by

$$r = (p - p_o)/(p_{max} - p_o) \qquad \text{(IV.8)}$$

where p is the particle momentum, $p_o$ is the cut-off momentum ($p_o$ equals 650 MeV for the muons and hadrons and 400 MeV for the electrons), and $p_{max}$ is the maximum momentum kinematically allowed in $\tau$ decay assuming properties IV.3. The corrected coplanarity angle distribution for all the anomalous events is shown in Figure 8(d).

Figure 8 also shows the distributions expected for heavy lepton production and decay. We again assume the properties IV.3 and a mix of $e\nu_e\nu_\tau$, $\mu\nu_\mu\nu_\tau$, $\nu_\tau\pi$ and $\nu_\tau\rho$ decay modes as given in Table III. The data are consistent with the heavy lepton hypothesis.

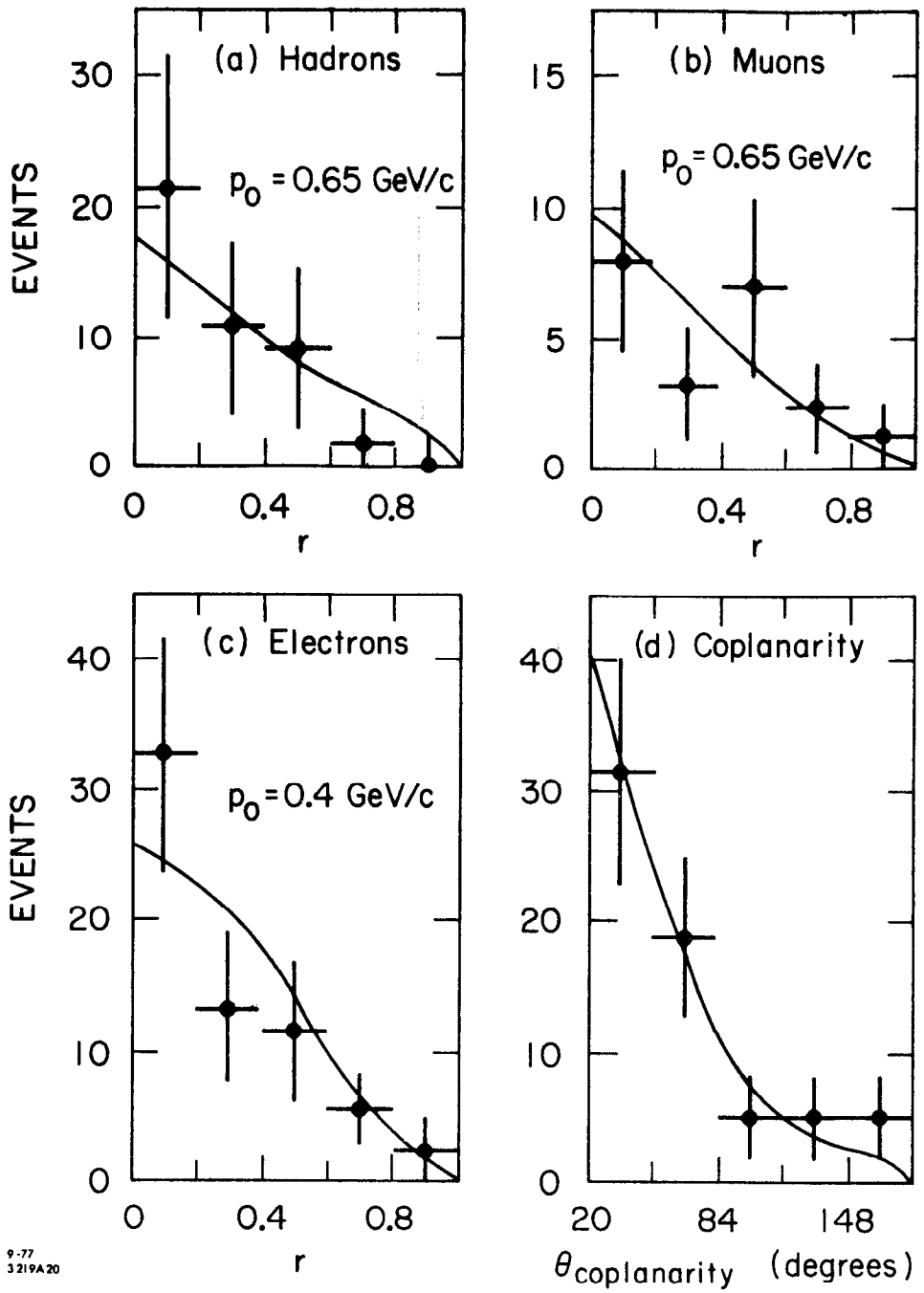


Fig. 8. The distributions for the momentum variable r (defined in the text) for a) the hadrons, b) the muons, and c) the electrons in the $e\mu$, eh and $eh\gamma$ events. Data from the three energy regions have been combined. Shown in d) is the coplanarity angle distribution for these two-prong anomalous electron events. The curves show the distributions expected for heavy lepton production and decay under the assumptions discussed in the text. The curves are normalized to the total number of entries in each plot.

A word of caution is in order. In our measurements of $B_e$ and $B_h$ and in the comparison of our data with the results expected from $\tau$ production and decay we have assumed that the heavy lepton is the only source of the two-prong anomalous electron events. Thus we have ignored a possible contribution from semi-leptonic decays of charmed particles.

D. Multiprong Events

We now consider the multihadronic events in which:

(1) a charged particle with momentum greater than 400 MeV/c enters the lead glass wall, and

(2) two or more additional charged particles are observed in the detector.

The events which pass these cuts are tabulated in Table VII. We show for each energy region the number of multiprong events with a particle identified as an electron in the lead glass wall. Also shown is the expected number of background events due to hadron misidentification and to electrons from converted photons or Dalitz decays with one member of the $e^+e^-$ pair undetected.[35] We attribute the electron signal above background to a non-conventional source. Correcting the number of electron candidate events for background, solid angle and identification efficiency of the lead glass wall, and detection efficiency for the other prongs, we calculate the cross section for multiprong events with an anomalous electron of momentum greater than 400 MeV/c. This is listed in the last column of Table VII. We observe a substantial anomalous electron signal in all four energy regions.

TABLE VII

Multiprong Events

See text for event selection. The last column lists the cross section $\sigma(e, p > 400\ MeV/c)$ for multiprong events with an anomalous electron of momentum p greater than 400 MeV/c.

| Center of mass energy range (GeV) | Number of electron candidate events | Number of expected background events | $\sigma(e, p > 400\ MeV/c)$ in multiprong events (nb) |
|---|---|---|---|
| 3.76-3.79[$\psi(3772)$] | 54 | 21 | 0.94 ± 0.33 |
| 4.15 | 55 | 17 | 1.29 ± 0.44 |
| 4.4-5.7 | 111 | 40 | 0.86 ± 0.25 |
| 6.4-7.4 | 165 | 63 | 0.54 ± 0.14 |
| Total | 385 | 141 | |

The corrected momentum distributions for the anomalous electrons at the $\psi(3772)$ and at the higher energies are shown in Figures 9 and 10. For comparison we show electron momentum spectra from D meson production (in the indicated production channels) with subsequent decay into $Ke\nu_e$ or $K^*e\nu_e$.[36]

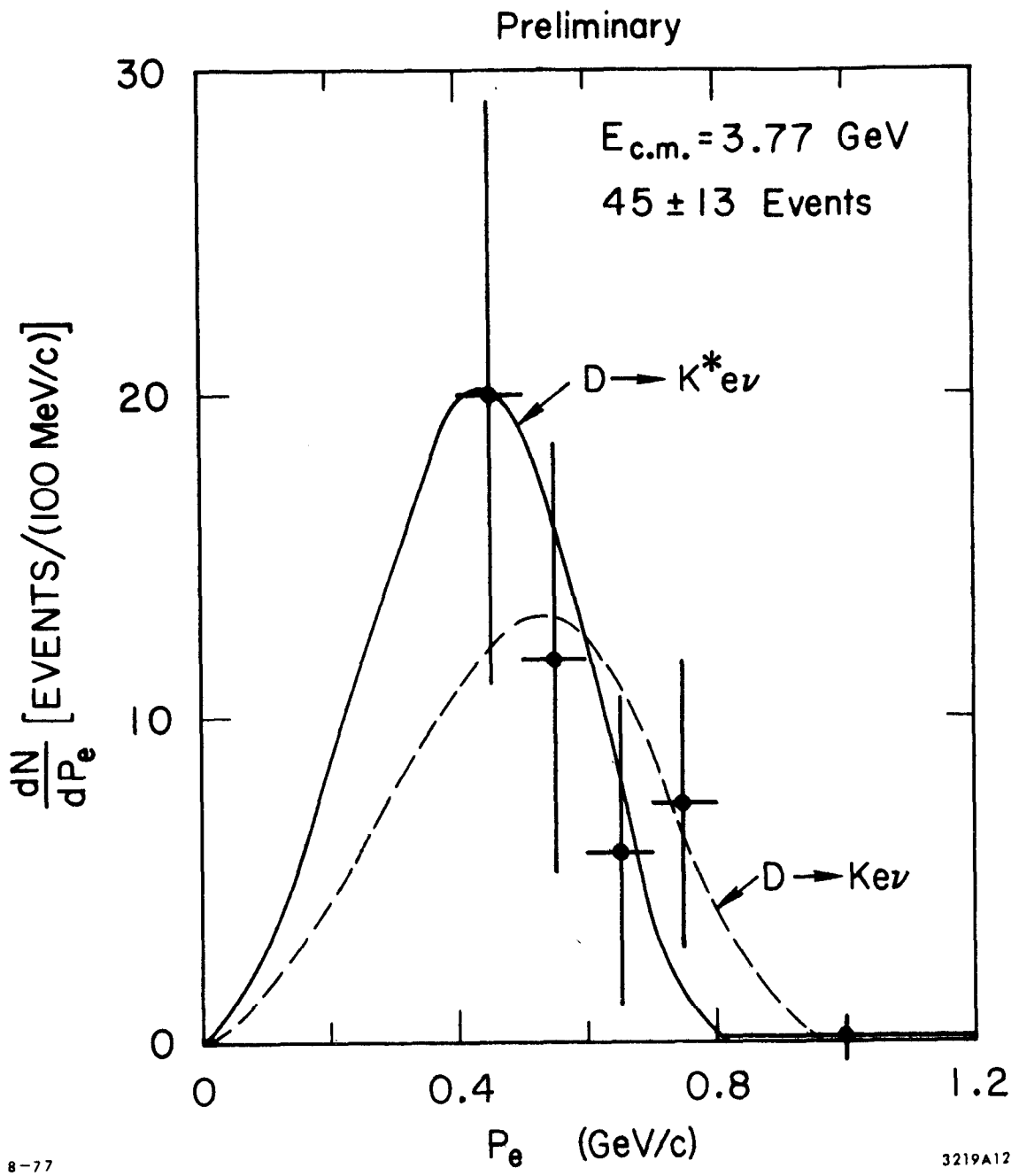


Fig. 9. The momentum spectrum above 400 MeV/c for the anomalous electrons produced in multiprong events at the $\psi(3772)$. The curves show the electron spectra expected from D meson production in the reaction $e^+e^- \to D\bar{D}$ followed by the decay $D \to Ke\nu_e$ or $D \to K^*e\nu_e$. The curves are normalized above 400 MeV/c to the total number of events.

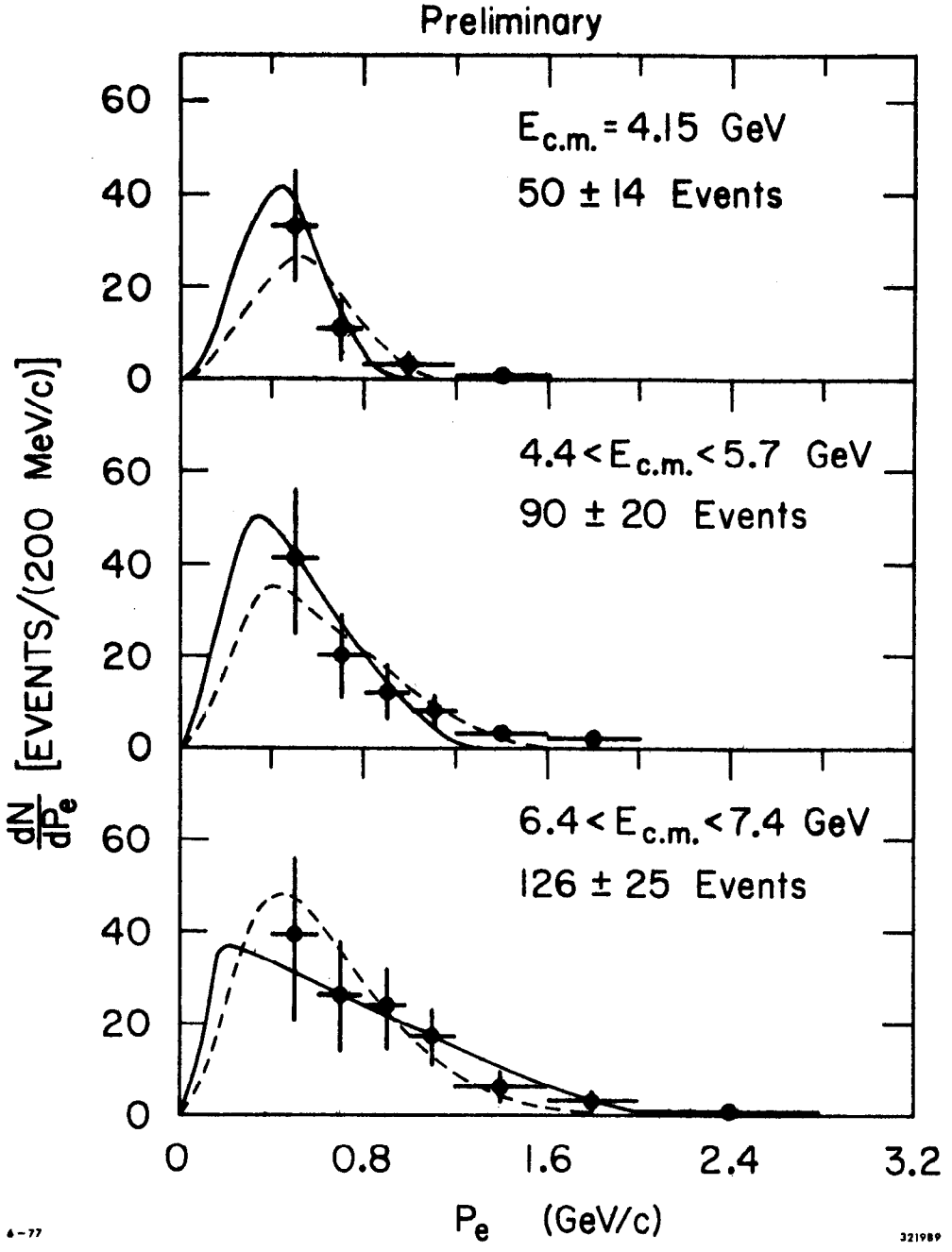


Fig. 10. The momentum spectra above 400 MeV/c for the anomalous electrons produced in multiprong events in three center of mass energy regions. The curves show the electron spectra expected from D meson production and decay. The decay modes are $D \to Ke\nu_e$ (dashed curve) or $D \to K^*e\nu_e$ (solid curve). The production channels are $e^+e^- \to 25\%\ D\bar{D}^* + 75\%\ D^*\bar{D}^*$ at $E_{c.m.} = 4.15$ GeV; $D^*\bar{D}^*$ for $4.4 < E_{c.m.} < 5.7$ GeV; $D^*\bar{D}^*$ with $D \to K^*e\nu_e$ and $D^*\bar{D}^*\pi\pi$ with $D \to Ke\nu_e$ for $6.4 < E_{c.m.} < 7.4$ GeV. The curves are normalized above 400 MeV/c to the total number of events.

Assuming the anomalous electron signal in the multiprong events arises from the production and decay of charmed particles,[37] as discussed in Section IV.A, we can estimate an average branching ratio $B_{c \to e}$ for charmed particles into electrons. We write:

$$B_{c \to e} = R(e)/2R(\text{charm}) \qquad \text{(IV.9)}$$

where R(e) is the anomalous electron production cross section in multiprong events divided by $\sigma_{\mu\mu}$ and R(charm) is the cross section for production of a pair of charmed particles, also divided by $\sigma_{\mu\mu}$. To evaluate R(e) we need to correct our measured electron cross section for the part of the electron spectrum which falls below our cut-off value of 400 MeV/c. For an estimate of this correction factor we use the curves shown in Figures 9 and 10, with an average over the $Ke\nu_e$ and $K^*e\nu_e$ decay modes. To evaluate R(charm) we assume:

$$R(\text{charm}) = R - R(\tau) - R(\text{old}) \qquad \text{(IV.10)}$$

where $R(\tau)$ is the contribution to R from $e^+e^- \to \tau^+\tau^-$ and R(old) is the constant R value for $e^+e^-$ → hadrons below charm threshold. We take $M(\tau) = 1.9$ GeV/$c^2$ and R(old) = 2.6.

Table VIII lists our values for R(e), R(charm) and $B_{c \to e}$, and Figure 11 shows $B_{c \to e}$ as a function of center of mass energy.

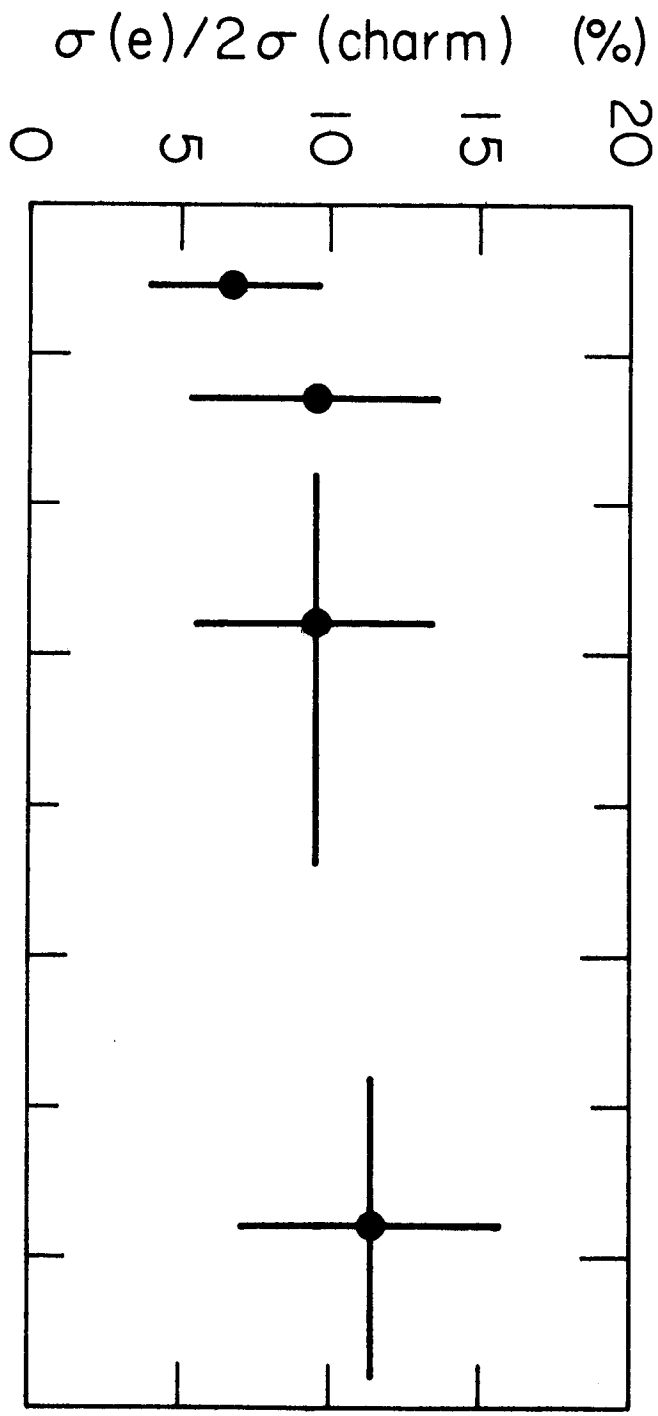


Fig. 11. $B_c \to e$ (defined in the text) vs. the center of mass energy.

TABLE VIII

Listed are the cross sections divided by $\sigma_{\mu\mu}$ for anomalous electron production in multiprong events [R(e)] and for the production of a pair of charmed particles [R(charm)]. $B_{c \to e}$ = R(e)/2R(charm).

| Center of mass energy range (GeV) | R(e) | R(charm) | $B_{c \to e}$ (%) |
|---|---|---|---|
| 3.76 - 3.79 [$\psi$(3772)] | 0.25 ± 0.09 | 1.82 ± 0.26 | 6.8 ± 2.9 |
| 4.15 | 0.40 ± 0.16 | 2.1 ± 0.4 | 9.5 ± 4.2 |
| 4.4 - 5.7 | 0.36 ± 0.13 | 1.9 ± 0.4 | 9.5 ± 4.0 |
| 6.4 - 7.4 | 0.41 ± 0.13 | 1.8 ± 0.4 | 11.4 ± 4.4 |

The value of $B_{c \to e}$ at the $\psi$(3772) is our estimate of the branching ratio for D mesons into electrons, averaged over the neutral and charged D's.[38] At the higher energies $B_{c \to e}$ may include contributions from other particle decays such as the F charmed meson or the charmed baryons.

V. A Brief Summary

We conclude with a brief summary of our experimental results.

(1) We observe a new resonance [$\psi$(3772)] in $e^+e^- \to$ hadrons with a mass of 3772 ± 6 MeV/$c^2$ and which decays into $D\bar{D}$.

(2) We measure the D masses to be:

$$M_{D^o} = 1863.3 \pm 0.9 \text{ MeV}/c^2$$

and

$$M_{D^+} = 1868.3 \pm 0.9 \text{ MeV}/c^2$$

with

$$M_{D^+} - M_{D^o} = 5.0 \pm 0.8 \text{ MeV}/c^2 \quad .$$

(3) We observe the decay mode $D^{\pm} \to K_s \pi^{\pm}$ and measure the D production angular distribution in $e^+e^- \to \psi(3772) \to D\bar{D}$ (it is consistent with the hypothesis of zero spin for the D mesons).

(4) We observe anomalous electron production in two-prong events which is consistent with the heavy lepton hypothesis. Assuming these events come only from $\tau$ production and decay we measure

$$B(\tau \to e\nu_e\nu_\tau) = (22.4 \pm 5.5)\%$$

and

$$B(\tau \to \text{charged hadron} + \text{neutrals}) = (45 \pm 19)\%$$

(5) We observe the production of anomalous electrons in multiprong events. Assuming these events come from the production and decay of charmed particles we estimate the average branching ratio for charmed particles into electrons to be about 10%.

Finally, I gratefully acknowledge the considerable effort of my colleagues on the Lead Glass Wall Collaboration that has been required to obtain the results given here.

REFERENCES AND FOOTNOTES

1. P.A. Rapidis et al., Phys. Rev. Lett. 39, 526(1977).

2. G.J. Feldman, SLAC report number SLAC-PUB-2000 (1977); I. Peruzzi et al., SLAC report number SLAC-PUB-2012 (1977).

3. A. Barbaro-Galtieri et al., SLAC report number SLAC-PUB-1976 (1977).

4. The members of the Lead Glass Wall Collaboration are: J.M. Dorfan, G.J. Feldman, G. Hanson, J.A. Jaros, B.P. Kwan, A.M. Litke, D. Lüke, J.F. Martin, M.L. Perl, I. Peruzzi, M. Piccolo, T.P. Pun, P.A. Rapidis, D.L. Scharre (Stanford Linear Accelerator Center and Department of Physics, Stanford University); A. Barbaro-Galtieri, R. Ely, J.M. Feller, A. Fong, P. Lecomte, R.J. Madaras, T.S. Mast, M.T. Ronan, R.R. Ross, B. Sadoulet, T.G. Trippe, V. Vuillemin (Lawrence Berkeley Laboratory and Department of Physics, University of California at Berkeley); B. Gobbi, D.H. Miller, (Department of Physics and Astronomy, Northwestern University); S.I. Parker, D.E. Yount (Department of Physics and Astronomy, University of Hawaii).

5. J.-E. Augustin et al., Phys. Rev. Lett. 34, 233(1975); G.J. Feldman and M.L. Perl, Phys. Rep. 19C, 233(1975), Appendix A; F. Vannucci et al., Phys. Rev. D15, 1814(1977).

6. Some low statistics measurements covering this region are reported in H.L. Lynch, Proceedings of the International Conference on the Production of Particles with New Quantum Numbers, University of Wisconsin, April 22-24, 1976, p. 20. A rise in $\sigma_{had}$ at the two standard deviation level was observed at 3.77 GeV.

7. Only statistical errors are shown. In addition there is an overall systematic error of $\pm$15% due mainly to an uncertainty in the detection efficiency of the apparatus.

8. J. Siegrist et al., Phys. Rev. Lett. 36, 700(1976).

9. J.-E. Augustin et al., Phys. Rev. Lett. 34, 764(1975).

10. J.D. Jackson, Nuovo Cimento 34, 1645(1964); A. Barbaro-Galtieri in Advances in Particle Physics, edited by R.L. Cool and R.L. Marshak (Wiley, New York), Vol. II, 1968.

11. A. M. Boyarski et al., Phys. Rev. Lett. 34, 1357(1975).

12. V. Lüth et al., Phys. Rev. Lett. 35, 1124(1975).

13. K. Lane and E. Eichten, Phys. Rev. Lett. 37, 477(1976).

14. E. Eichten et al., Phys. Rev. Lett. 34. 369(1975); Phys. Rev. Lett. 36, 500(1976).

15. G. Goldhaber et al., Phys. Rev. Lett. 37, 255(1976); I. Peruzzi et al., Phys. Rev. Lett. 37, 569(1976).

16. V. Lüth et al., SLAC report number SLAC-PUB-1947 (1977).

17. The spread in the beam energy is about 1 MeV, due to quantum fluctuations in synchrotron radiation. The long term monitoring of $E_B$ is done to better than 0.5 MeV.

18. This is a consistency argument; it does not prove the D mesons have zero spin. Higher spins may also have a $\sin^2\theta$ angular distribution. See H.K. Nguyen et al., Phys. Rev. Lett. 39, 262(1977) for additional experimental evidence on D and D* spin.

19. M.L. Perl et al., Phys. Rev. Lett. 35, 1489(1975).

20. M.L. Perl et al., Phys. Lett. 63B, 466(1976).

21. For reviews of the evidence see G. Flügge in Proc. of the V International Conference on Experimental Meson Spectroscopy (Northwestern University Boston, 1977), to be published; M.L. Perl in Proc. of the XII Rencontre de Moriond (Flaine, 1977), edited by Tran Thanh Van, R.M.I.E.M. Orsay, to be published.

22. M. Cavalli-Sforza et al., Phys. Rev. Lett. 36, 558(1976).

23. G. Snow, Phys. Rev. Lett. 36, 766(1976).

24. G.J. Feldman et al., Phys. Rev. Lett. 38, 117(1977).

25. M.L. Perl et al., SLAC report number SLAC-PUB-1997 (1977).

26. H. Meyer in Proceedings of the Orbis Scientiae - 1977 (Coral Gables 1977) to be published; V. Blobel in Proceedings of the XII Rencontre de Moriond (Flaine, 1977), edited by Tran Thanh Van, R.M.I.E.M. Orsay to be published; J. Burmester et al., DESY preprints DESY 77/24 and DESY 77/25 (1977).

27. R. Felst, paper presented at the Chicago Meeting of the American Physical Society (February 1977); W. Wallraff in Proceedings of the XII Rencontre de Moriond (Flaine, 1977), edited by Tran Thanh Van, R.M.I.E.M. Orsay, to be published.

28. For recent results from DORIS consult the report of U. Timm in these proceedings.

29. These values are consistent with the experimental results of reference 25.

30. The predictions are based on Y.S. Tsai, Phys. Rev. D4, 2821(1971) and H.B. Thacker and J.J. Sakurai, Phys. Lett. 36B, 103(1971) as discussed by G.J. Feldman in Proceedings of the 1976 Summer Institute on Particle Physics, (SLAC, Stanford, Calif., 1976); also issued as SLAC-PUB-1852 (1976).

31. W. Braunschweig et al., Phys. Lett. 63B, 471(1976).

32. J. Burmester et al., Phys. Lett. 64B, 369(1976).

33. The number of $e\mu\gamma$ events after correction for background and misidentification is consistent with zero and we will not discuss these further.

34. See Table III.

35. $e^+e^-$ pairs with both particles detected are eliminated by a cut on the opening angle between the particle in the lead glass wall and all other detected particles with the opposite charge. The only other significant source of background from conventional sources is the reaction $e^+e^- \to e^+e^-\gamma$ with the photon converting to a $e^+e^-$ pair. These events are easily identified and have been removed from the data sample.

36. We use the electron decay spectra from I. Hinchliffe and C.H. Llewellyn Smith, Nucl. Phys. B114, 45(1976).

37. These events may also arise them from the production and decay of heavy leptons. However, assuming that B($\tau \to$ three or more charged hadrons + neutrals) = 15%, we calculate that not more than 10% of the events can come from this source.

38. Assuming that the $\psi(3772)$ is a state of definite isospin (0 or 1) then $D^o$ and $D^+$ will be produced with equal probability except for factors dependent on the D mass. From the momentum dependent width given in II.3 we estimate the ratio of $D^o$ to $D^o$ or $D^+$ production on the $\psi(3772)$ to be $0.56 \pm 0.03$.